Inorganic Chemistry

Article

pubs.acs.org/IC

# Unusual Coordination for Plutonium(IV), Cerium(IV), and Zirconium(IV) in the Cationic Layered Materials $[M_2Te_4O_{11}]X_2$ (M = Pu, Ce, Zr; X = Cl, Br)

Jian Lin,[‡] Justin N. Cross,[‡] Juan Diwu,[‡] Matthew J. Polinski,[‡] Eric M. Villa,[‡] and Thomas E. Albrecht-Schmitt*[,†]

[†]Department of Chemistry and Biochemistry, Florida State University, Tallahassee, Florida 32306, United States

[‡]Department of Civil & Environmental Engineering & Earth Sciences and Department of Chemistry and Biochemistry, University of Notre Dame, 156 Fitzpatrick Hall, Notre Dame, Indiana 46556, United States

Supporting Information

**ABSTRACT:** Four isotypic cationic layered materials, $[Pu_2Te_4O_{11}]Cl_2$, $[Ce_2Te_4O_{11}]Cl_2$, $[Zr_2Te_4O_{11}]Cl_2$, and $[Zr_2Te_4O_{11}]Br_2$, have been prepared under hydrothermal conditions. Single crystal diffraction studies reveal that these materials possess cationic Pu/Ce/Zr tellurite layers with halides as interlamellar charge-balancing anions. The $Pu^{IV}$, $Ce^{IV}$, and $Zr^{IV}$ centers of the cationic layers exhibit a quite rare pentagonal bipyramid coordination environment.

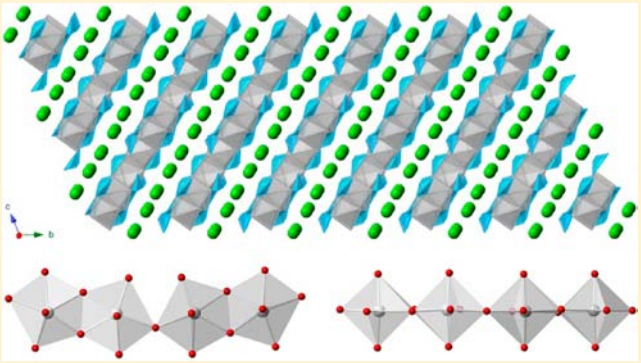

## INTRODUCTION

Many metal oxo-hydroxo anions are listed by the EPA as inorganic pollutants, and chromate and pertechnetate are inherent to the nuclear weapons complex legacy of the Cold War as well as to advanced nuclear fuel cycles.[1] Cationic extended materials with anion exchange capabilities can be utilized to sequester these anionic pollutants. Materials with extended structures are typically anionic in nature, and the charge is balanced by cations that fill the voids leading to an overall neutral charge.[2] Only a handful of inorganic materials with an extended cationic network charge balanced by isolated anions exist.[1] On the basis of the inorganic crystal structure database (ICSD), fewer than 100 cationic inorganic materials exist among 150,042 crystal structures. Cationic inorganic materials with anion exchange capabilities are much rarer. A series of layered double hydroxides (LDHs) have been reported that possess cationic layers and exchangeable interlamellar anions.[3] A number of cationic metal−organic frameworks (MOFs) materials with vast types of topologies that exhibit anion exchange have also been synthesized.[4] However, LDHs are of limited relatively low thermal stability, and MOFs are vulnerable to decomposition because of their organic linkers.[1,5] As a result, we are investigating the synthesis of inorganic cationic extended materials that are stable under environmentally relevant conditions with potential for trapping anions of concern. Our research efforts have successfully given rise to a complex thorium borate, NDTB-1, that possesses a super-tetrahedral cationic framework that selectively removes $TcO_4^-$ from nuclear waste streams despite the presence of large excesses of competing anions.[6]

We have recently undertaken a study of the solid-state chemistry of actinides, lanthanides, and transition metals using a variety of oxoanions, such as borate, tellurite, and phosphite. Borate and tellurite share a common property in that they both are highly polarizable and can possesses polymeric structures. Tellurite is of course very different from borate in that it possesses a stereochemically active lone pair of electrons on the $Te^{IV}$ centers that lead to a large variability in coordination environments and properties in this family of compounds. Tellurite anions can be further interconnected to form dimers, trimers, and polymeric structures, which enable a variety of unusual structures to form.[7] For example, novel infinite tellurite tubes with lone-pair self-containment have been reported.[8] Unusual uranyl tellurites containing $[Te_2O_6]^{4-}$ ions and three-dimensional (3D) networks have been observed in uranyl tellurites.[9] A new 3D $Te_7O_{17}^{6-}$ building unit has been discovered by our group.[10] Ok et al.'s and our studies suggest that the lone pair electrons of tellurites can push the oxygen atoms toward one side of the cation and create a highly distorted environment, making it an ideal component for synthesis of cationic extended materials.[10,11]

In addition, tellurites bind metals in a variety of ways leading to a rich study of the coordination chemistry of actinides,

**Received:** August 23, 2012
**Published:** October 17, 2012

   dx.doi.org/10.1021/ic301846g | *Inorg. Chem.* 2012, 51, 11949−11954

Table 1. Crystallographic Data for $[Pu_2Te_4O_{11}]Cl_2$, $[Ce_2Te_4O_{11}]Cl_2$, $[Zr_2Te_4O_{11}]Cl_2$, and $[Zr_2Te_4O_{11}]Br_2$

| compound | $[Pu_2Te_4O_{11}]Cl_2$ | $[Ce_2Te_4O_{11}]Cl_2$ | $[Zr_2Te_4O_{11}]Cl_2$ | $[Zr_2Te_4O_{11}]Br_2$ |
|---|---|---|---|---|
| formula mass | 1241.30 | 1037.54 | 939.74 | 1028.66 |
| color | green | yellow | colorless | yellow |
| Habit | tablet | tablet | tablet | tablet |
| space group | $P\bar{1}$ | $P\bar{1}$ | $P\bar{1}$ | $P\bar{1}$ |
| $a$ (Å) | 8.0505(16) | 8.1046 (19) | 7.7986(11) | 7.800(3) |
| $b$ (Å) | 9.488(3) | 9.5210(2) | 9.4173(13) | 9.529(3) |
| $c$ (Å) | 10.433(2) | 10.4230(3) | 10.3257(15) | 10.563(5) |
| $\alpha$ (deg) | 109.289(3) | 108.537(2) | 111.031(2) | 112.513(4) |
| $\beta$ (deg) | 108.169(2) | 108.932(2) | 107.958(2) | 106.483(5) |
| $\gamma$ (deg) | 98.374(3) | 98.327 (2) | 98.476(2) | 99.473(3) |
| $V$ (Å$^3$) | 686.7(3) | 693.2(3) | 644.28(16) | 661.6(5) |
| $Z$ | 2 | 2 | 2 | 2 |
| $T$ (K) | 100(2) | 100(2) | 100(2) | 100(2) |
| $\lambda$ (Å) | 0.71073 | 0.71073 | 0.71073 | 0.71073 |
| maximum $2\theta$ (deg.) | 27.590 | 27.700 | 27.570 | 27.610 |
| $\rho_{calcd}$ (g cm$^{-3}$) | 6.004 | 4.971 | 4.844 | 5.164 |
| $\mu$ (Mo K$\alpha$) (cm$^{-1}$) | 182.77 | 151.63 | 109.56 | 163.05 |
| $R(F)$ for $F_o^2 > 2\sigma(F_o^2)^a$ | 0.0504 | 0.0436 | 0.0423 | 0.0450 |
| $R_w$ $(F_o^2)^b$ | 0.1181 | 0.0959 | 0.1023 | 0.1081 |

$^a R(F) = \sum||F_o| - |F_c||/\sum|F_o|$. $^b R_w(F_o^2) = [\sum[w(F_o^2-F_c^2)^2]/\sum wF_o^4]^{1/2}$.

lanthanides, and transition metals. Both $Pu^{IV}$ and $Ce^{IV}$ can be seven, eight, or nine coordinated by oxygen, yielding different coordination geometries based on square antiprism, hexagonal bipyramid, tricapped trigonal prism, trigonal dodecahedra, distorted dodecahedra, and so forth.[12] $Zr^{IV}$ can be six and eight coordinated by oxygen with octahedral, and dodecahedral environments, respectively.[13] Seven coordinate $Zr^{IV}$ with oxygen is relatively rare.

Herein, we present a series of isotypic metal tellurites, $[M_2Te_4O_{11}]X_2$ (M = Pu, Ce, Zr; X = Cl, Br), with cationic layered structures and an unusual coordination environment of the metal centers.

## EXPERIMENTAL SECTION

**Synthesis.** $CeCl_3$ (99.5%, Alfa-Aesar), $ZrCl_4$ (98%, Alfa-Aesar), $ZrBr_4$ (99%, Alfa-Aesar), and $TeO_2$ (99.99%, Alfa-Aesar), were all used as received. Weapons-grade plutonium (94% $^{239}$Pu, 6% $^{240}$Pu) in the form of $PuCl_3$ was used as received from the Los Alamos National Laboratory (LANL). Reactions were run in PTFE-lined Parr 4749 autoclaves with a 23 mL internal volume for the cerium/zirconium and with 10 mL internal volume autoclaves for plutonium. Distilled and Millipore filtered water with resistance of 18.2 MΩ·cm was used in all reactions.

***Caution!*** *$^{239}$Pu ($t_{1/2}$ = 24,065 years), and $^{240}$Pu ($t_{1/2}$ = 6,537 years) represent serious health risks owing to their α and γ emission. All studies with plutonium were conducted in a laboratory dedicated to studies on transuranium elements. This laboratory is located in a nuclear science facility and is equipped with HEPA filtered hoods and negative pressure gloveboxes that are ported directly into the hoods. A series of counters continually monitor radiation levels in the laboratory. The laboratory is licensed by the Nuclear Regulatory Commission. All experiments were carried out with approved safety operating procedures. All free-flowing solids are worked with in gloveboxes, and products are only examined when coated with either water or Krytox oil and water. There are significant limitations in accurately determining yield with plutonium compounds because this requires drying, isolating, and weighing a solid, which poses certain risks, as well as manipulation difficulties given the small quantities employed in the reactions.*

**$[Pu_2Te_4O_{11}]Cl_2$.** $PuCl_3$ (0.029 mM, 0.0100 g), $TeO_2$ (0.0589 mM, 0.0094 g), and water (300 μL) were loaded into a 10 mL autoclave. The autoclave was sealed and heated to 230 °C in a box furnace for 3 days. The autoclave was then cooled to room temperature at a rate of 5 °C/h. The products were rinsed with DI water, and pale green tablets were isolated.

**$[Ce_2Te_4O_{11}]Cl_2$.** $CeCl_3$ (1 mM, 0.2465 g), $TeO_2$ (1 mM, 0.1596 g), and water (2 mL) were loaded into a 23 mL PTFE-lined autoclave linear. The autoclave was sealed and heated to 230 °C for 3 days followed by slow cooling to room temperature at a rate of 5 °C/h. The products were washed with DI water to remove soluble solids, followed by rinsing with methanol. The products consisted of light yellow tablet crystals of $[Ce_2Te_4O_{11}]Cl_2$.

**$[Zr_2Te_4O_{11}]X_2$ (X = Cl$^-$ or Br$^-$).** $ZrX_4$ (1 mM, 0.2330 g for $ZrCl_4$, 0.4108 g for $ZrBr_4$), $TeO_2$ (1 mM, 0.1596 g), and water (2 mL) were loaded into a 23 mL PTFE-lined autoclave linear. The autoclave was sealed and heated to 230 °C in a box furnace for 3 days. The autoclave was then cooled to room temperature at a rate of 5 °C/h. The products were washed with DI water to remove soluble solids, followed by rinsing with methanol. $[Zr_2Te_4O_{11}]X_2$ crystallizes as tablets. $[Zr_2Te_4O_{11}]Cl_2$ is colorless and $[Zr_2Te_4O_{11}]Br_2$ is light yellow. Photographs of all three sets of crystals can be found in the Supporting Information.

**Crystallographic Studies.** Single crystals of $[M_2Te_4O_{11}]X_2$ were mounted on CryoLoops with Krytox oil and optically aligned on a Bruker APEXII Quazar X-ray diffractometer using a digital camera. Initial intensity measurements were performed using an IμSX-ray source, a 30 W microfocused sealed tube (MoKα, λ = 0.71073 Å) with high-brilliance and high-performance focusing Quazar multilayer optics. Standard APEXII software was used for determination of the unit cells and data collection control. The intensities of reflections of a sphere were collected by a combination of four sets of exposures (frames). Each set had a different φ angle for the crystal, and each exposure covered a range of 0.5° in ω. A total of 1464 frames were collected with an exposure time per frame of 20 to 60 s, depending on the crystal. The SAINT software was used for data integration including Lorentz and polarization corrections. Semiempirical absorption corrections were applied using the program SADABS or TWINABS. Selected crystallographic information is listed in Table 1. Atomic coordinates and additional structural information are provided in the Supporting Information (CIFs).

**UV−Vis−NIR Spectroscopy.** UV−vis−NIR data were acquired from single crystals using a Craic Technologies microspectrophotometer. Crystals were placed on quartz slides under Krytox oil, and the data was collected from 200 to 1400 nm.


dx.doi.org/10.1021/ic301846g | Inorg. Chem. 2012, 51, 11949−11954

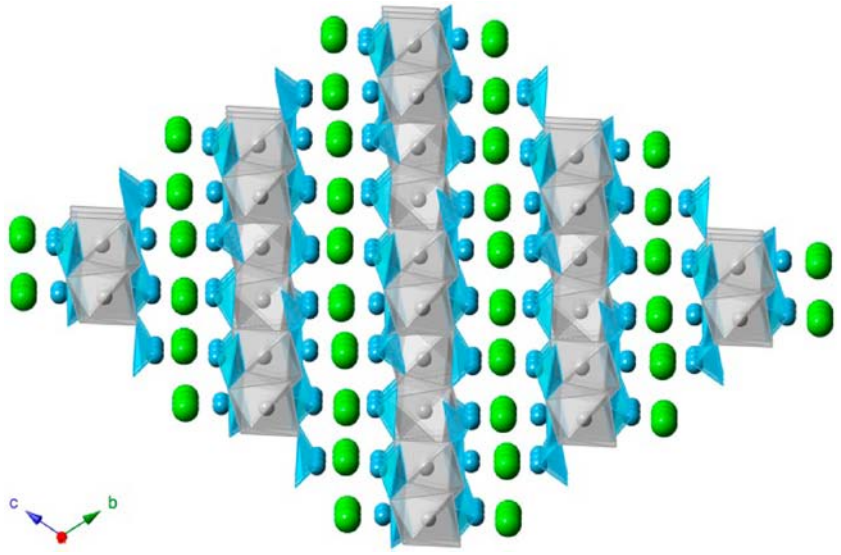


**Figure 1.** View of $[M_2Te_4O_{11}]X_2$ (M = Pu, Ce, Zr, X = Cl, Br) parallel to the [*bc*] plane showing the cationic layered structure extending down the *a* axis and halides anions filling between layers. Metal polyhedra are shown in gray, tellurites in blue, and halides anions in green.

## RESULTS AND DISCUSSION

**Synthesis.** All four compounds were synthesized using metal halides and tellurium dioxide under hydrothermal conditions. The stoichiometry of the reactants is critical. For example, a lower ratio (1:2) of $CeCl_3/TeO_2$ results in generating of $[Ce_2Te_7O_{17}]Cl_2$ as the main product instead of $[Ce_2Te_4O_{11}]Cl_2$. All of compounds contain tetravalent metals even though $[Pu_2Te_4O_{11}]Cl_2$ and $[Ce_2Te_4O_{11}]Cl_2$ were synthesized from $Pu^{III}/Ce^{III}$ halides. $Pu^{IV}$ is the favored valence under ambient condition and oxygen from air can easily oxidize $Pu^{III}$ to $Pu^{IV}$.[14] However, the redox potential for $Ce^{IV}/Ce^{III}$ is 1.28 V/NHE in 1 M HCl and $Ce^{III}$ is the preferred valence state under acidic condition.[15] The oxidation of $Ce^{III}$ to $Ce^{IV}$ under hydrothermal condition can be attributed to complexation by tellurite, the different pH conditions, and a possible solubility-driven mechanism. These solubility-driven redox changes have been proposed in our previous studies.[12a,g,16]

**Structures and Topological Descriptions.** Single crystal X-ray diffraction reveals that all compounds are isotypic materials with an inorganic cationic layered structure. To the best of our knowledge, $[Pu_2Te_4O_{11}]Cl_2$ not only represents the first transuranium cationic structure, but also the first known plutonium tellurite halide compound. Additionally, $[Ce_2Te_4O_{11}]Cl_2$, $[Zr_2Te_4O_{11}]Cl_2$, and $[Zr_2Te_4O_{11}]Br_2$ are the first cerium/zirconium cationic layered materials. Figure 1 depicts the cationic layers extending along the *a* axis. The structure consists of a cationic Pu/Ce/Zr tellurite layer with halides as interlamellar charge-balancing anions. The distance between each layer is 4.242 Å for $[Pu_2Te_4O_{11}]Cl_2$, 4.328 Å for $[Ce_2Te_4O_{11}]Cl_2$, 4.352 Å for $[Zr_2Te_4O_{11}]Cl_2$, and 4.410 Å for $[Zr_2Te_4O_{11}]Br_2$, respectively. The variance of the layer distances is due to the different ionic radii of the metal ions ($Pu^{IV} \approx Ce^{IV} > Zr^{IV}$) and halides ($Br^- > Cl^-$).[17] The larger the metal ion is, the longer the M−O bond would be.[18] Extended M−O bonds expand the layer size, in the meanwhile, squeeze interlamellar space. Similarly, the smaller the halide is, the shorter the layer distance would be.

The $[M_2Te_4O_{11}]^{2-}$ layer is composed of two crystallographically independent metal atoms and two types of tellurite anions, forming a tellurite-metal-tellurite sandwich structure (cf. Figure 2a). Within the metal-oxo sheet, the crystallographically unique polyhedra edge-share with themselves to form dimers and the different dimers corner-share alternatively, resulting the formation of the one-dimensional (1D) metal ribbons (cf. Figure 2b). In the tellurite sheet, there are two different building units, $TeO_3^{2-}$ and $Te_3O_8^{4-}$, which are dark-blue and light-blue colored in Figure 2c. For $TeO_3^{2-}$, each $Te^{4+}$ bonds to three oxygen atoms with bond distance ranging from 1.828(14) Å to 1.911(12) Å. For $Te_3O_8^{4-}$, the central $Te^{4+}$ is bonded to four oxygen atoms and the other two $Te^{4+}$ atoms are bonded to three oxygen atoms. The Te−O bond distances range from 1.817(6) Å to 2.151(9) Å (cf. Table 2). The distances of bridging Te−O bond [Te(4)−O(5) and Te(4)−O(8)] are larger than 2 Å, and the terminal Te−O bond lengths are smaller than 2 Å. All oxygen atoms donated from tellurite anions either corner-share or edge-share with the metal centers, connecting with the metal ribbons into the two-dimensional (2D) $[M_2Te_4O_{11}]^{2-}$ layer.

The cationic layered structure of these materials suggested the possibility for anion exchange behavior. Anion exchange of $[Ce_2Te_4O_{11}]Cl_2$ and $[Zr_2Te_4O_{11}]X_2$ crystals were conducted with common anions ($F^-$, $Cl^-$, $Br^-$, $I^-$, $SO_4^{2-}$, $NO_3^-$, $MnO_4^-$) and measured by energy-dispersive X-ray spectroscopy (EDS). Unfortunately, the interlamellar halides do not exchange with other anions. The nonbonded electron pairs on $Te^{4+}$ point into the layer interfaces, forming electrostatic interactions with the halides (cf. Figure 1). Te atoms retain their valence shell s-electrons via the inert pair effect and effectively block halide mobility.[1] Thus, the halides are locked within the layers, which is likely the reason $[Ce_2Te_4O_{11}]Cl_2$ and $[Zr_2Te_4O_{11}]X_2$ lack the ability to anion exchange. This locking effect has been observed in a mixed-metal oxychlorides $Te_4M_3O_{15}{\cdot}Cl$ and inorganic cationic frameworks $[Ce_2Te_7O_{17}]X_2$ (X = $Cl^-$ or $Br^-$).[10,11] $Te_4M_3O_{15}{\cdot}Cl$ and $[Ce_2Te_7O_{17}]X_2$ exhibit 3D cationic tunnel framework and current structures are 2D layered. One thing in common is that the all $Te^{4+}$ centers are in asymmetric coordination environments attributable to their nonbonded electron pair. The nonbonded electron pairs on $Te^{4+}$ point into the center of the channel or layer interfaces, where the halide anion resides. A thermal ellipsoid plot for the $TeO_3$, and $Te_3O_8$


dx.doi.org/10.1021/ic301846g | *Inorg. Chem.* 2012, 51, 11949−11954

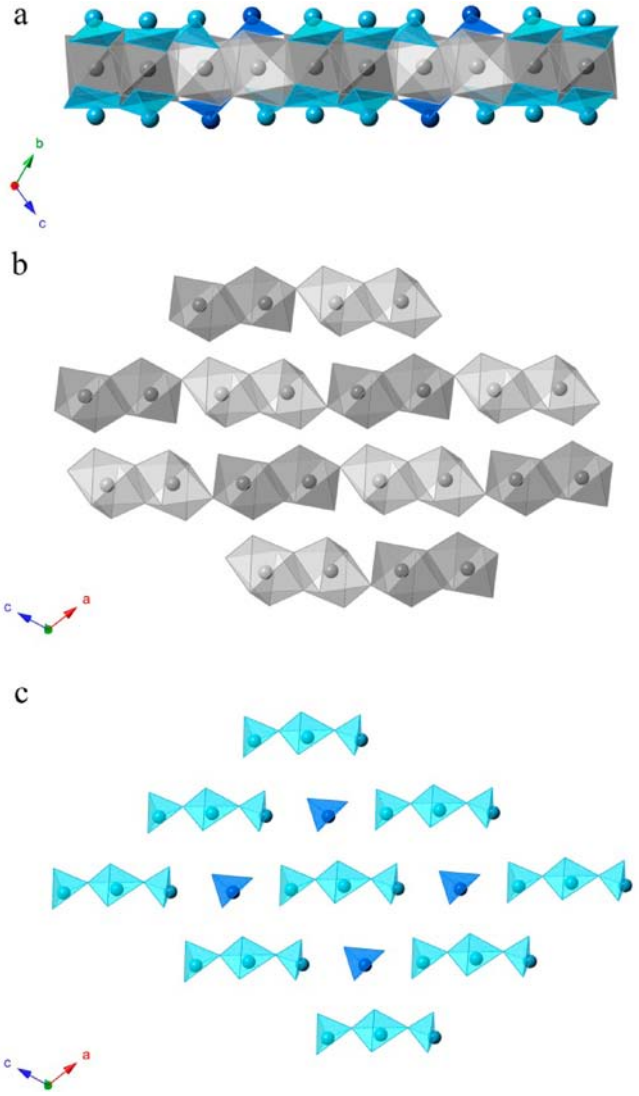


**Figure 2.** (a) Crystallographic view of one $[M_2Te_4O_{11}]^{2-}$ layer along the *a* axis. (b) Depiction of the metal-oxo sheet topology. Metal dimers (1) are shown in light-gray, metal dimers (2) are in dark-gray. (c) Depiction of the tellurite sheet topology. $TeO_3^{2-}$ tetrahedra are in dark-blue and $Te_3O_8^{4-}$ polymers are in light-blue.

polyhedra are shown in the Supporting Information. Another possibility is that halides do not favor exchange with other anions because of their stability in the structure. Other anions with less electrostatic interactions with the framework or higher mobility might be more likely to exchange.

Another key feature of these $[M_2Te_4O_{11}]X_2$ compounds is the coordination environment of the $Pu^{IV}$, $Ce^{IV}$, and $Zr^{IV}$ centers (Figure 3). In $[M_2Te_4O_{11}]X_2$, novel pentagonal bipyramid $Pu^{IV}$, $Ce^{IV}$, and $Zr^{IV}$ centers were discovered (cf. Figure 2 and Table 2). Pentagonal bipyramid geometry is very common for neptunyl, uranyl, and can sometimes be found in Th and Eu.[19] However, it is quite rare in low oxidation state lanthanides and actinides. In $[M_2Te_4O_{11}]X_2$, $M^{IV}$ polyhedra edge-share to form dimers, and all oxygen atoms bound to $M^{IV}$ are donated from tellurite anions. The capping oxygen has relatively short M−O bond lengths ranging from 2.142(9) to 2.179(9) Å for $[Pu_2Te_4O_{11}]Cl_2$, 2.136(8) to 2.173(8) Å for $[Ce_2Te_4O_{11}]Cl_2$, 2.005(6) to 2.032(6) Å for $[Zr_2Te_4O_{11}]Cl_2$, and 2.006(6) Å to 2.032(5) Å for $[Zr_2Te_4O_{11}]Br_2$. The M−O

**Table 2. Selected Bond Distances for $[Pu_2Te_4O_{11}]Cl_2$, $[Ce_2Te_4O_{11}]Cl_2$, $[Zr_2Te_4O_{11}]Cl_2$, and $[Zr_2Te_4O_{11}]Br_2$[a]**

| | Pu (Cl) | Ce (Cl) | Zr (Cl) | Zr (Br) |
|---|---|---|---|---|
| M(1)−O(4) | 2.160(9) | 2.173(8) | 2.030(6) | 2.023(5) |
| M(1)−O(10) | 2.179(9) | 2.136(8) | 2.025(6) | 2.012(6) |
| M(1)−O(3) | 2.170(14) | 2.207(9) | 2.072(7) | 2.069(7) |
| M(1)−O(8) | 2.406(10) | 2.438(8) | 2.227(6) | 2.246(6) |
| M(1)−O(9) | 2.427(9) | 2.295(8) | 2.239(6) | 2.243(6) |
| M(1)−O(9) | 2.286(9) | 2.398(8) | 2.154(6) | 2.171(6) |
| M(1)−O(11) | 2.357(9) | 2.402(8) | 2.282(6) | 2.266(6) |
| M(2)−O(1) | 2.142(9) | 2.159(7) | 2.005(6) | 2.006(6) |
| M(2)−O(7) | 2.161(9) | 2.167(8) | 2.032(6) | 2.032(5) |
| M(2)−O(2) | 2.270(11) | 2.181(9) | 2.071(7) | 2.069(7) |
| M(2)−O(5) | 2.410(9) | 2.419(8) | 2.240(6) | 2.250(6) |
| M(2)−O(6) | 2.366(9) | 2.284(8) | 2.245(6) | 2.254(6) |
| M(2)−O(6) | 2.310(9) | 2.420(8) | 2.141(6) | 2.166(6) |
| M(2)−O(11) | 2.350(9) | 2.398(8) | 2.274(6) | 2.271(6) |
| Te(1)−O(1) | 1.840(9) | 1.842(8) | 1.834(6) | 1.839(6) |
| Te(1)−O(2) | 1.911(12) | 1.848(9) | 1.849(7) | 1.855(7) |
| Te(1)−O(3) | 1.828(14) | 1.849(9) | 1.851(7) | 1.858(7) |
| Te(2)−O(4) | 1.835(9) | 1.828(8) | 1.817(6) | 1.830(5) |
| Te(2)−O(5) | 2.005(8) | 1.923(8) | 1.950(6) | 1.972(6) |
| Te(2)−O(6) | 1.890(9) | 1.912(8) | 1.909(6) | 1.895(6) |
| Te(3)−O(7) | 1.835(10) | 1.828(8) | 1.822(6) | 1.826(5) |
| Te(3)−O(8) | 1.924(9) | 1.943(8) | 1.962(6) | 1.978(6) |
| Te(3)−O(9) | 1.918(10) | 1.902(8) | 1.898(6) | 1.896(6) |
| Te(4)−O(5) | 2.049(8) | 2.109(8) | 2.066(6) | 2.076(6) |
| Te(4)−O(8) | 2.151(9) | 2.066(7) | 2.067(6) | 2.077(6) |
| Te(4)−O(10) | 1.824(9) | 1.847(7) | 1.821(6) | 1.837(5) |
| Te(4)−O(11) | 1.943(10) | 1.911(8) | 1.947(6) | 1.950(6) |

[a]M(1)−O(4), M(1)−O(10), M(2)−O(1), and M(2)−O(7) are the metal-capping oxygen bonds. Te(4)−O(5) and Te(4)−O(8) are the bridging Te−O bonds.

bond distances within the pentagonal plane range from 2.170(14) Å to 2.427(9) Å, 2.181(9) Å to 2.438(8) Å, 2.071(7) Å to 2.282(6) Å, and 2.069(7) Å to 2.271(6) Å in $[Pu_2Te_4O_{11}]Cl_2$, $[Ce_2Te_4O_{11}]Cl_2$, $[Zr_2Te_4O_{11}]Cl_2$, and $[Zr_2Te_4O_{11}]Br_2$, respectively (cf. Table 2). Bond valence calculations indicate all metals are tetravalent, which agree with the charge balanced formulas.[20] These isotypic $[M_2Te_4O_{11}]X_2$ compounds provide us an additional opportunity to discern differences in bond distances between $Pu^{IV}$, $Ce^{IV}$, and $Zr^{IV}$. The average M−O lengths are 2.3(1) Å, 2.3(1) Å, 2.1(1) Å, 2.1(1) Å for $[Pu_2Te_4O_{11}]Cl_2$, $[Ce_2Te_4O_{11}]Cl_2$, $[Zr_2Te_4O_{11}]Cl_2$, and $[Zr_2Te_4O_{11}]Br_2$, respectively, which suggest the larger the metal ion is, the longer the M−O bond would be.[18] This result also suggests there are no measurable differences between $Pu^{IV}$−O bonds and $Ce^{IV}$−O bonds, which matches our previous study.[12b]

**UV−Vis−NIR Absorption Spectroscopy.** The absorption spectra for $[Pu_2Te_4O_{11}]Cl_2$, $[Ce_2Te_4O_{11}]Cl_2$, $[Zr_2Te_4O_{11}]Cl_2$, and $[Zr_2Te_4O_{11}]Br_2$ were obtained from single or twinned crystals of each compound and are shown in Figure 4a. The existence of $Pu^{IV}$ in $[Pu_2Te_4O_{11}]Cl_2$ can be confirmed by the UV−vis-NIR spectrum (cf. Figure 4b). The $^5F_2$ + $^5I_6$ peaks centered near 1100 nm are signature peaks of $Pu^{IV}$. At wavelengths less than 900 nm, the transitions are due to multiple *J* states and have not been deconvoluted, but the transitions match well with the spectra reported by Carnall.[21] $Ce^{IV}$ and $Zr^{IV}$ have empty 4f and 4d orbitals, respectively, and do not exhibit any f-f or d-d transitions in the absorption


dx.doi.org/10.1021/ic301846g | *Inorg. Chem.* 2012, 51, 11949−11954

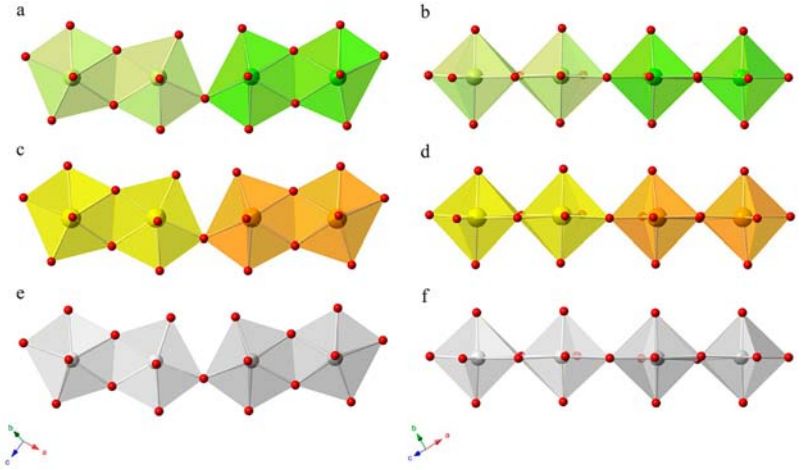


**Figure 3.** Top (a, c, e) and side (b, d, f) views of the pentagonal bipyramid $M^{IV}$ chains. The $Pu^{IV}$ centers are green spheres, the $Ce^{IV}$ centers are yellow/orange spheres, the $Zr^{IV}$ centers are gray spheres, and the oxygen atoms are red spheres.

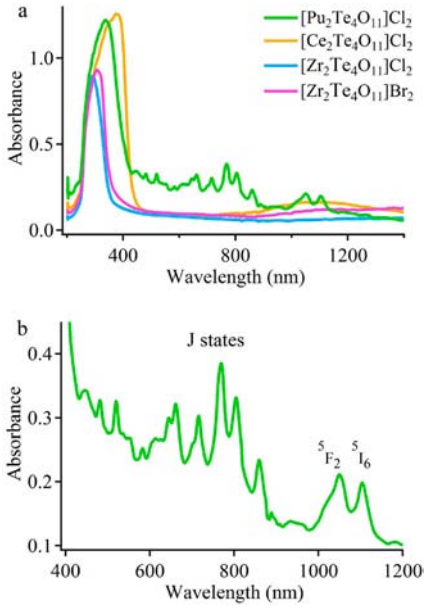


**Figure 4.** (a) UV–vis–NIR spectra of $[Pu_2Te_4O_{11}]Cl_2$, $[Ce_2Te_4O_{11}]Cl_2$, $[Zr_2Te_4O_{11}]Cl_2$, and $[Zr_2Te_4O_{11}]Br_2$. (b) UV–vis–NIR spectra of $[Pu_2Te_4O_{11}]Cl_2$ showing the assigned peaks for different f-f transitions (The $^5F_2$ + $^5I_6$ peaks centered at 1100 nm are signature peaks of the $Pu^{IV}$; at wavelengths <909 nm, multiple *J* values contribute).

spectra. The peaks ranging from 200 to 300 nm are ascribed to the Te–O charge transfer based on the measurement of $TeO_2$ crystal.

## CONCLUSIONS

A series of inorganic cationic layered materials have been synthesized under hydrothermal conditions. $[Pu_2Te_4O_{11}]Cl_2$, $[Ce_2Te_4O_{11}]Cl_2$, $[Zr_2Te_4O_{11}]Cl_2$, and $[Zr_2Te_4O_{11}]Br_2$ represent the first plutonium/cerium/zirconium cationic layered materials with $[Pu_2Te_4O_{11}]Cl_2$ representing the first plutonium tellurite. The $Pu^{IV}$, $Ce^{IV}$, and $Zr^{IV}$ centers of these materials also exhibit an unusual pentagonal bipyramid coordination environment. To obtain cationic extended materials with anion exchange ability, anions with less electrostatic interactions with the framework and higher mobility will be incorporated in future studies.

## ASSOCIATED CONTENT

### Supporting Information

X-ray crystallographic files in CIF, photographs of the crystals, and ORTEP for the $MO_7$, $TeO_3$, and $Te_3O_8$ polyhedra are shown. This material is available free of charge via the Internet at http://pubs.acs.org.

## AUTHOR INFORMATION

### Corresponding Author

*E-mail: talbrechtschmitt@gmail.com.

### Notes

The authors declare no competing financial interest.

## ACKNOWLEDGMENTS

This material is based upon work supported as part of the Materials Science of Actinides, an Energy Frontier Research Center funded by the U.S. Department of Energy, Office of Science, Office of Basic Energy Sciences under Award Number DE-SC0001089. This work was supported by a Chinese Scholarship Council Graduate Fellowship to J.L.

## REFERENCES

(1) Oliver, S. R. J. *Chem. Soc. Rev.* **2009**, *38*, 1868–1881.
(2) Rives, V. *Layered double hydroxides: present and future*; Nova Science Publishers: New York, 2001.
(3) (a) Geng, F.; Xin, H.; Matsushita, Y.; Ma, R.; Tanaka, M.; Izumi, F.; Iyi, N.; Sasaki, T. *Chem.—Eur. J.* **2008**, *14*, 9255–9260. (b) McIntyre, L. J.; Jackson, L. K.; Fogg, A. M. *Chem. Mater.* **2007**, *20*, 335–340. (c) Geng, F.; Matsushita, Y.; Ma, R.; Xin, H.; Tanaka, M.; Izumi, F.; Iyi, N.; Sasaki, T. *J. Am. Chem. Soc.* **2008**, *130*, 16344–16350. (d) Goulding, H. V.; Hulse, S. E.; Clegg, W.; Harrington, R. W.; Playford, H. Y.; Walton, R. I.; Fogg, A. M. *J. Am. Chem. Soc.* **2010**, *132*, 13618–13620. (e) Hindocha, S. A.; McIntyre, L. J.; Fogg, A. M. *J. Solid State Chem.* **2009**, *182*, 1070–1074.
(4) (a) Fei, H.; Pham, C. H.; Oliver, S. R. J. *J. Am. Chem. Soc.* **2012**, *134*, 10729–10732. (b) Fei, H.; Rogow, D. L.; Oliver, S. R. J. *J. Am. Chem. Soc.* **2010**, *132*, 7202–7209. (c) Rogow, D. L.; Russell, M. P.; Wayman, L. M.; Swanson, C. H.; Oliver, A. G.; Oliver, S. R. J. *Cryst. Growth Des.* **2010**, *10*, 823–829. (d) Fei, H.; Oliver, S. R. J. *Dalton Trans.* **2010**, *39*, 11193–11200.
(5) Wang, Q.; O'Hare, D. *Chem. Rev.* **2012**, *112*, 4124–4155.
(6) (a) Wang, S.; Alekseev, E. V.; Juan, D. W.; Casey, W. H.; Phillips, B. L.; Depmeier, W.; Albrecht-Schmitt, T. E. *Angew. Chem., Int. Ed.* **2010**, *49*, 1057–1060. (b) Wang, S.; Yu, P.; Purse, B. A.; Orta, M. J.;

Diwu, J.; Casey, W. H.; Phillips, B. L.; Alekseev, E. V.; Depmeier, W.; Hobbs, D. T.; Albrecht-Schmitt, T. E. *Adv. Funct. Mater.* **2012**, *22*, 2241−2250.
(7) Mao, J.-G.; Jiang, H.-L.; Kong, F. *Inorg. Chem.* **2008**, *47*, 8498−8510.
(8) Johnston, M. G.; Harrison, W. T. A. *J. Am. Chem. Soc.* **2002**, *124*, 4576−4577.
(9) Almond, P. M.; McKee, M. L.; Albrecht-Schmitt, T. E. *Angew. Chem., Int. Ed.* **2002**, *41*, 3426−3429.
(10) Lin, J.; Diwu, J.; Cross, J. N.; Villa, E. M.; Albrecht-Schmitt, T. E. *Inorg. Chem.* **2012**, *51*, 10083−10085.
(11) Ok, K. M.; Halasyamani, P. S. *Inorg. Chem.* **2004**, *43*, 4248−4253.
(12) (a) Diwu, J.; Wang, S.; Liao, Z.; Burns, P. C.; Albrecht-Schmitt, T. E. *Inorg. Chem.* **2010**, *49*, 10074−10080. (b) Diwu, J.; Nelson, A.-G. D.; Wang, S.; Campana, C. F.; Albrecht-Schmitt, T. E. *Inorg. Chem.* **2010**, *49*, 3337−3342. (c) Cross, J. N.; Villa, E. M.; Wang, S.; Diwu, J.; Polinski, M. J.; Albrecht-Schmitt, T. E. *Inorg. Chem.* **2012**, *51*, 8419−8424. (d) Diwu, J.; Good, J. J.; Di, S. V. H.; Albrecht-Schmitt, T. E. *Eur. J. Inorg. Chem.* **2011**, 1374−1377. (e) Diwu, J.; Nelson, A.-G. D.; Albrecht-Schmitt, T. E. *Comments Inorg. Chem.* **2010**, *31*, 46−62. (f) Wang, S.; Villa, E. M.; Diwu, J.; Alekseev, E. V.; Depmeier, W.; Albrecht-Schmitt, T. E. *Inorg. Chem.* **2011**, *50*, 2527−2533. (g) Sykora, R. E.; Deakin, L.; Mar, A.; Skanthakumar, S.; Soderholm, L.; Albrecht-Schmitt, T. E. *Chem. Mater.* **2004**, *16*, 1343−1349. (h) Salvadó, M. A.; Pertierra, P.; Trobajo, C.; García, J. R. *J. Am. Chem. Soc.* **2007**, *129*, 10970−10971.
(13) (a) Pinnavaia, T. J.; Fay, R. C. *Inorg. Chem.* **1968**, *7*, 502−508. (b) Toth, L. M.; Quist, A. S.; Boyd, G. E. *J. Phys. Chem.* **1973**, *77*, 1384−1388. (c) Yi; Zhang, Q.-F.; Lam, T. C. H.; Chan, E. Y. Y.; Williams, I. D.; Leung, W.-H. *Inorg. Chem.* **2005**, *45*, 328−335. (d) Kato, C. N.; Shinohara, A.; Hayashi, K.; Nomiya, K. *Inorg. Chem.* **2006**, *45*, 8108−8119.
(14) Edelstein, N. M.; Fuger, J.; Morss, L. R. *The Chemistry of the Actinide and Transactinide Elements*; Springer: New York, 2010.
(15) Maverick, A. W.; Yao, Q. *Inorg. Chem.* **1993**, *32*, 5626−5628.
(16) Diwu, J.; Wang, S.; Good, J. J.; DiStefano, V. H.; Albrecht-Schmitt, T. E. *Inorg. Chem.* **2011**, *50*, 4842−4850.
(17) Shannon, R. *Acta Crystallogr., Sect. A: Found. Crystallogr.* **1976**, *32*, 751−767.
(18) Minasian, S. G.; Boland, K. S.; Feller, R. K.; Gaunt, A. J.; Kozimor, S. A.; May, I.; Reilly, S. D.; Scott, B. L.; Shuh, D. K. *Inorg. Chem.* **2012**, *51*, 5728−5736.
(19) (a) Volkringer, C.; Henry, N.; Grandjean, S.; Loiseau, T. *J. Am. Chem. Soc.* **2011**, *134*, 1275−1283. (b) Jin, G. B.; Skanthakumar, S.; Soderholm, L. *Inorg. Chem.* **2012**, *51*, 3220−3230. (c) Ling, J.; Ward, M.; Burns, P. C. *J. Solid State Chem.* **2011**, *184*, 401−404. (d) Daly, S. R.; Girolami, G. S. *Inorg. Chem.* **2010**, *49*, 4578−4585. (e) Salvadó, M. A.; Pertierra, P.; Castro, G. R.; Trobajo, C.; García, J. R. *Inorg. Chem.* **2008**, *47*, 1246−1248. (f) Forbes, T. Z.; Burns, P. C. *J. Solid State Chem.* **2007**, *180*, 106−112. (g) Forbes, T. Z.; Burns, P. C. *J. Solid State Chem.* **2005**, *178*, 3445−3452.
(20) (a) Brese, N. E.; O'Keeffe, M. *Acta Crystallogr., Sect. B* **1991**, *47*, 192−197. (b) Roulhac, P. L.; Palenik, G. J. *Inorg. Chem.* **2002**, *42*, 118−121.
(21) (a) Carnall, W. T.; Fields, P. R.; Pappalar, R. G. *J. Chem. Phys.* **1970**, *53*, 2922−2938. (b) Carnall, W. T.; Liu, G. K.; Williams, C. W.; Reid, M. F. *J. Chem. Phys.* **1991**, *95*, 7194−7203.